Localizing transcripts to single cells suggests an important role of uncultured deltaproteobacteria in the termite gut hydrogen economy

Adam Z. Rosenthal[a,1], Xinning Zhang[a,1], Kaitlyn S. Lucey[a], Elizabeth A. Ottesen[a], Vikas Trivedi[b], Harry M. T. Choi[b], Niles A. Pierce[b,c], and Jared R. Leadbetter[a,2]

[a]Ronald and Maxine Linde Center for Global Environmental Science, [b]Department of Bioengineering, and [c]Department of Computing and Mathematical Sciences, California Institute of Technology, Pasadena, CA 91125

Edited by James M. Tiedje, Michigan State University, East Lansing, MI, and approved August 13, 2013 (received for review April 29, 2013)

Identifying microbes responsible for particular environmental functions is challenging, given that most environments contain an uncultivated microbial diversity. Here we combined approaches to identify bacteria expressing genes relevant to catabolite flow and to locate these genes within their environment, in this case the gut of a "lower," wood-feeding termite. First, environmental transcriptomics revealed that 2 of the 23 formate dehydrogenase (FDH) genes known in the system accounted for slightly more than one-half of environmental transcripts. FDH is an essential enzyme of H_2 metabolism that is ultimately important for the assimilation of lignocellulose-derived energy by the insect. Second, single-cell PCR analysis revealed that two different bacterial types expressed these two transcripts. The most commonly transcribed FDH in situ is encoded by a previously unappreciated deltaproteobacterium, whereas the other FDH is spirochetal. Third, PCR analysis of fractionated gut contents demonstrated that these bacteria reside in different spatial niches; the spirochete is free-swimming, whereas the deltaproteobacterium associates with particulates. Fourth, the deltaproteobacteria expressing FDH were localized to protozoa via hybridization chain reaction-FISH, an approach for multiplexed, spatial mapping of mRNA and rRNA targets. These results underscore the importance of making direct vs. inference-based gene–species associations, and have implications in higher termites, the most successful termite lineage, in which protozoa have been lost from the gut community. Contrary to expectations, in higher termites, FDH genes related to those from the protozoan symbiont dominate, whereas most others were absent, suggesting that a successful gene variant can persist and flourish after a gut perturbation alters a major environmental niche.

acetogenesis | RNA-Seq | microfluidic digital PCR

A large body of work in microbial ecology is centered on documenting gene and organism diversity into large catalogs. The development of tools that unambiguously identify environmentally active organisms within these immense catalogs has lagged, however. Phylogenetic inventories of ribosomal RNA and physiology-relevant genes are often constructed to examine the evolutionary relationship and full diversity of bacteria and their many functional roles in nature. Linking species marker genes for given microbes in the environment with genes for important ecological functions has proven more challenging. Gene inventory-based studies often attempt to assign functional genes to their encoding organisms by inference, for example, based on parallels in the branching order of the respective phylograms prepared from different inventories, noting the positions of genes belonging to reference organisms on those same trees. Phylogenetic inference is limited, however, because genetic transfers can occur across phylogenetic lines of descent, and is even less predictive if the availability of reference organisms for internal calibration of phylograms is limited.

In the present study, gene inventories and community-wide transcriptional profiles were combined with single-cell analyses and in situ assays to address such matters directly. We interrogated a tiny, yet complex environment that accommodates robust, stable, and species-rich microbial communities—the hindgut of a wood-feeding lower termite, *Zootermopsis nevadensis* (1).

Termites and their gut microbiota digest lignocellulose, the most abundant natural composite material on Earth. For some time now, it has been known that a key activity in this nutritional mutualism involves the bacterial conversion of H_2 + CO_2, generated during wood polysaccharide fermentation, into acetate in a process called CO_2-reductive acetogenesis (2, 3). The acetate originating from CO_2-reductive acetogenesis fuels up to one-fifth to one-third of the termites' carbon and energy needs (4, 5). The H_2 concentration and turnover measured in termite hindguts is among the highest recorded in any biological system, and H_2 gas is the central free intermediate during lignocellulose degradation (6). Thus, identifying the microbes involved in H_2 + CO_2 metabolism during acetogenesis or other H_2-using reactions, and localizing their activity in situ, has great relevance in understanding both host nutrition and the global carbon cycle.

All H_2 + CO_2 acetogenic bacteria isolated from termites to date have been members of the bacterial phyla *Spirochetes* or *Firmicutes* (4, 7, 8). Gene-based community analyses have led to a guiding hypothesis that some, most, or all of the contributors to gut acetogenesis may be spirochetes, many of which have not yet been cultivated. In contrast, there has been no support for an important homoacetogenic role of endospore-forming *Firmicutes* species isolated at low abundances from termites or their close relatives (6, 8–12). The hypothesis that spirochetes may account for most or all of termite gut acetogenesis remains largely

Significance

Most environments host a poorly understood microbial diversity. In recent years, work on gene inventories and metagenomics has revealed much about the microbial species and metabolic genes that may be present in situ; however, connecting microbial species with environmental function has lagged. Here a combination of emerging single-cell and other approaches revealed the gut microbes that may catalyze a key activity in their termite hosts. The results implicate a previously unappreciated deltaproteobacterium living on a gut protist.

Author contributions: A.Z.R., X.Z., E.A.O., H.M.T.C., N.A.P., and J.R.L. designed research; A.Z.R., X.Z., K.S.L., E.A.O., V.T., and H.M.T.C. performed research; A.Z.R., X.Z., K.S.L., E.A.O., V.T., H.M.T.C., N.A.P., and J.R.L. analyzed data; and A.Z.R., X.Z., N.A.P., and J.R.L. wrote the paper.

The authors declare no conflict of interest.

This article is a PNAS Direct Submission.

Data deposition: 16S rRNA gene sequences, FDH sequences, and FTHFS sequences have been deposited in the GenBank database (accession nos. JX974519, GU563433–GU563485, GQ922349–GQ922449, and JX974463–JX974518).

[1]A.Z.R. and X.Z. contributed equally to this work.

[2]To whom correspondence should be addressed. E-mail: jleadbetter@caltech.edu.

This article contains supporting information online at www.pnas.org/lookup/suppl/doi:10.1073/pnas.1307876110/-/DCSupplemental.

MICROBIOLOGY

untested, however, because much of the available data are based on accumulated indirect phylogenetic inferences, relying heavily on the limited availability of cultivated homoacetogenic species for use as requisite internal references.

Here we have focused on the analysis of genes and transcripts for hydrogenase-linked formate dehydrogenase (FDH) and, to a lesser extent, formyl-tetrahydrofolate synthetase (FTHFS) (6, 9–11, 13, 14), which together catalyze the first and second steps of the folate branch of the CO_2-reductive acetogenesis pathway: $H_2 + CO_2$ => formate, and formate + THF => formyl-tetrahydrofolate (15). We also note that FDH genes may play roles in other processes that consume or generate $H_2 + CO_2$, for example, as a follow-up to the pyruvate-formate lyase reaction in enterics (16), during purine fermentation (17), and during interspecies formate transfer (18). Of these reactions, FDH is known to be important to symbiosis only in CO_2-reductive acetogenesis; however, in principle, all of the reactions are relevant, inasmuch as both H_2 and formate serve as substrates for CO_2-reductive acetogenesis (15). To move beyond phylogenetic prediction and to physically identify the microbial species responsible for $H_2 + CO_2$ metabolism in termite guts, we sought to circumvent the limitation of indirect inference using a combination of gene-based approaches (*SI Appendix*, Fig. S1).

Results

Community Transcripts of Two Genes Essential to $H_2 + CO_2$ Metabolism Are Dominated by Only a Few Phylotypes. Leveraging the predictive power of existing hydrogenase-linked FDH (*fdhF*) and FTHFS gene inventories (9, 11, 19), gut environmental metatranscriptomic data were used to identify highly expressed alleles for each of these functional gene types. High-throughput cDNA sequencing (RNA-Seq) is increasingly used to quantify transcriptional intensity. In environmental transcriptomics, previous knowledge of endogenous gene sequences may serve as a "scaffold" onto which sequence fragments are mapped. Total gut RNA was extracted from the gut tracts of fresh field-collected and laboratory-maintained specimens of *Z. nevadensis* workers, converted to cDNA, and sequenced (*Materials and Methods* and *SI Appendix*, Table S1), generating datasets of 14,043,698 (field specimens) and 13,913,270 (laboratory specimens) 37-mer reads. To increase read density, the sample from freshly collected specimens was sequenced more extensively, providing an additional 217,687,073 50-mer reads. All three libraries were combined in silico to compile a large dataset (~245 million reads). Taking into account ribosomal RNA (~90–95% total RNA) and total RNA from protozoa, which dominate as much as 90% of the volume of the gut lumen (1), the number of reads corresponding to bacterial mRNA transcripts was ~2,500,000.

To examine the entire dataset for evidence of gut transcription of FDH alleles, comparisons were made to a scaffold library containing 44 known *fdh*F alleles representing 23 phylotypes previously inventoried in *Z. nevadensis* gut. Only reads perfectly matching a scaffold were counted as positive hits, and these were considered unique only when they could be mapped solely to alleles corresponding to a single FDH-deduced phylotype. A total of 920 unique reads mapped onto the *Z. nevadensis fdhF* scaffold dataset (Table 1). More than 40% of these reads ($n = 381$) mapped to a single phylotype, ZnD2sec (selenocysteine containing FDH; GenBank accession no. GU563467), aligning to 207 distinct locations along the reference gene sequence. The remaining 539 reads mapped to 18 different deduced FDH phylotypes: in order of abundance (Table 1), ZnHcys (cysteine containing FDH; GenBank accession no. GQ922420), Zn2cys (GenBank accession no. GQ922431), alleles identical to the known *fdh*F_{Sec} and *fdh*F_{Cys} genes of cultivated strain *Treponema primitia* ZAS-2 (GenBank accession nos. ADJ19611 and ADJ19610) (11), and 14 other "phylogenetically *Treponeme*-like" FDH genes.

The foregoing results verify that the expression of previously inventoried functional genes can be reliably detected in total environmental RNA pools using either specific or degenerate PCR primers targeting particular gene types. The RNA-Seq mapping approach proved to be highly precise for the system at hand; comparison of all reads with an additional 180 FDH genotypes identified from guts of insects other than *Z. nevadensis,* as well as all those available in public databases (*SI Appendix*, Table S2), yielded only 17 additional hits (1.8%) (*SI Appendix*, Table S3). The most highly expressed phylotypes generally were equally represented across both field and laboratory specimens (*SI Appendix*, Table S3). Interestingly, ZnHcys, the second most highly expressed variant in samples originating from freshly collected field specimens, was not detected in the RNA-Seq library from laboratory-maintained specimens. Further analysis of this was beyond the scope of this study.

As an internal check of consistency, using different methods, the relative abundances of the top alleles were confirmed via cDNA libraries and quantitative RT-PCR (qPCR) (*Materials and Methods* and *SI Appendix*, Table S3). RNA-Seq reads were also mapped to libraries of FTHFS gene variants (*SI Appendix*, Table S4). FTHFS variant P37-7A (33.6%) and an FTHFS sequence identical to that encoded by the cultivated homoacetogen *T. primitia* ZAS-2 (24.5%) were the most highly expressed phylotypes, together accounting for 58% of all reads. The observation that the fourth and fifth most highly expressed FDHs and the second most highly expressed FTHFS are identical to those from termite isolate *T. primitia* ZAS-2, which is known to encode two FDHs (13), directly demonstrates the relevance of this species to CO_2-reductive acetogenesis activity in the gut environment. This species has served as a representative symbiont in studies over the past decade (8, 10).

Microfluidic Digital PCR Identifies Termite Gut Spirochetes Encoding Highly Expressed FDH Phylotypes. Subsequent efforts focused on learning more about the species identity and nature of the bacteria encoding the two most highly expressed hydrogenase-linked FDH phylotypes, ZnD2sec and Zn2cys, in laboratory-maintained insects. We turned to microfluidic multiplex digital-PCR single-particle analysis, an approach that has been used to identify the rRNA phylotypes of termite gut bacteria associated with specific metabolic or phage genes (14, 20). This platform works by sequestering individual particles from a diluted microbial community into 6.25-nL chambers, wherein multiplex qPCR is performed using oligonucleotides targeting both functional genes of interest and ribosomal small subunit (SSU rRNA) genes. The PCR products generated in chambers containing positive signal(s) can be retrieved manually and subsequently analyzed. Here degenerate PCR primer and probe sets targeting either FDH or FTHFS were used in concert with those targeting the SSU

Table 1. *Z. nevadensis* gut community FDH gene transcription

Phylotype	FDH type	RNA-Seq unique hits	% of total hits
ZnD2sec	*fdh*F_{sec}	381	41.41
ZnHcys	*fdh*F_{cys}	129	14.02
Zn2cys	*fdh*F_{cys}	84	9.13
T. primitia	*fdh*F_{sec}	67	7.28
T. primitia	*fdh*F_{cys}	60	6.52
Zn61sec	*fdh*F_{sec}	41	4.46
ZnF7sec	*fdh*F_{sec}	28	3.04
ZnB5sec	*fdh*F_{sec}	27	2.93
ZnB9cys	*fdh*F_{cys}	24	2.61
ZnLsec	*fdh*F_{sec}	20	2.17
ZnB8sec	*fdh*F_{sec}	13	1.41
ZnD3cys	*fdh*F_{cys}	11	1.20
ZnC6sec	*fdh*F_{sec}	8	0.87
Zn36sec RT	*fdh*F_{sec}	7	0.76
Zn51sec	*fdh*F_{sec}	6	0.65
ZnPcys	*fdh*F_{cys}	5	0.54
Zn75cysRT	*fdh*F_{cys}	4	0.43
Zn72secRT	*fdh*F_{sec}	4	0.43
ZnH8cys	*fdh*F_{cys}	1	0.11

rRNA genes from all bacteria. From this, robust associations between several FDH genes and bacterial species were drawn. The Zn2cys FDH variant, the third most abundant transcript in fresh field-collected insects and the second most abundant in laboratory-maintained specimens, was strongly associated with a spirochetal ribotype, *Treponema* genomovar ZnR11 (GenBank accession no. JX571935) (*SI Appendix*, Fig S2).

Using these same methods, we found that this spirochete also colocalized with the gene for ZNF7sec, the seventh most highly expressed FDH in field-collected specimens (Table 1 and *SI Appendix*, Fig. S1), suggesting that, as is known for cultivated strains of the bacterium *T. primitia* (11, 13), this organism encodes both seleno and cysteinyl variants of FDH. *Treponema* genomovar ZnR11 also associated with a specific FTHFS allele (*SI Appendix*, Fig. S2), the fourth most highly expressed FTHFS in situ, accounting for ∼8% of hits to the FTHFS scaffold library (*SI Appendix*, Table S4), a finding corroborated by a previously published FTHFS expression profile (6). The microfluidic platform successfully linked four different genes to a single genomovar, a feat not previously accomplished using digital PCR. Several other FDH and FTHFS phylotypes were also successfully linked to specific SSU rRNA genes, all of which were spirochetal (*SI Appendix*, Figs. S2 and S3).

The ZnD2sec FDH Gene Is Overrepresented Within the Gut Particulate Fraction, Which Contains Wood Particles and Protozoa. Curiously, all initial attempts to forge links between either the most highly expressed FTHFS phylotype (P37-7A) or the most highly expressed FDH phylotype (ZnD2sec) and specific SSU rRNA genes or their complementary functional genes were unsuccessful. We investigated why ZnD2sec, the most highly expressed FDH in situ, was not captured in these initial microfluidic trials. One possibility was that the source organism encoding ZnD2sec, although highly active, might be insufficiently abundant in gut contents to enable detection in microfluidic assays. To examine this possibility, we prepared libraries of selenocysteine FDH ($fdhF_{Sec}$) genes using standard PCR, low-degeneracy primers optimized to minimize primer bias (19), and total gut DNA preparations. The ZnD2sec FDH gene accounted for 64% of the $fdhF_{Sec}$ clones in the resulting libraries from total gut DNA, implying that it is perhaps the most abundant $fdhF_{Sec}$-encoding member of the community. However, termite gut bacteria are known to strongly attach to the gut wall (21, 22) and to associate with the surfaces or insides of gut protozoa (23), in addition to being free-swimming. Through the microfluidic device loading method, larger wood particles, protozoal particles, gut epithelial tissues, and other aggregates were routinely excluded from our initial microfluidic protocols, to prevent channel clogging in the device. This might explain the lack of amplification of the ZnD2sec gene from density-clarified samples.

To examine this possibility, qPCR was performed on both particle-associated fractions and density-clarified fractions of gut luminal contents. Primers specific for either the ZnD2sec gene or the $fdhF_{sec}$ of the spirochete *T. primitia* ZAS-2 were used. The *T. primitia* gene was 6.5-fold more abundant in the density-clarified luminal fluid compared with the particle-associated fraction, whereas the ZnD2sec was 86-fold more abundant in the particle-associated fraction. These results are consistent with the idea that the spirochete *T. primitia* ZAS-2 is free-swimming, whereas ZnD2sec is associated with either wood particles or protozoa. These findings largely explain the initial failure to amplify ZnD2sec using microfluidics (*SI Appendix*, Table S5).

ZnD2sec, the Most Highly Transcribed Hydrogenase-Linked FDH Gene in both Laboratory and Field-Collected Specimens of *Z. nevadensis*, Is Encoded by a Protist-Associated Deltaproteobacterium. To identify cells carrying the ZnD2sec gene, we performed microfluidic digital PCR on homogenized particulate fractions to detect positive amplification of ZnD2sec. In multiplex reactions, the ZnD2sec gene was coamplified with the same SSU rRNA gene (GenBank accession no. JX974519) in five of seven wells that returned sequences for both genes (*SI Appendix*, Table S8). Sequence analysis of wells with coamplification revealed that the ZnD2sec FDH gene is encoded by a novel deltaproteobacterium (Fig. 1 and *SI Appendix*, Table S3).

Deltaproteobacteria encompass many diverse subgroups and physiotypes, including anaerobic dissimilatory sulfate-, sulfur-, iron-, and manganese-reducing bacteria, as well as strictly oxygen-respiring predatory myxobacteria and bdellovibrios. At least one species of deltaproteobacteria is known to be capable of bona-fide CO_2-reductive, acetogenic growth (24). The not-yet-cultivated phylotype encoding ZnD2sec is distinct from any characterized deltoproteobacteria in the literature, but clusters with marker sequences from several not-yet-cultivated organisms resident in diverse termite gut tracts (Fig. 1). The closest cultivated and described species belong to the order Desulfarculales, specifically *Desulfarculus baarsii,* a poorly studied bacterium capable of sulfate reduction as well as CO_2 fixation into acetate via the acetyl-CoA pathway (25). Although *D. baarsii* was originally named *Desulfovibrio baarsii*, neither it nor the sequences related to the organism encoding ZnD2sec are closely related to members of the genus *Desulfovibrio*, several species of which inhabit termite guts, including on the surface of certain protozoa, but none of which are homoacetogenic (26).

Our findings imply a major role for deltaproteobacteria in the $H_2 + CO_2$ economy of termite hindgut communities. They also contradict initial phylogenetic inference, which in the absence of the proper reference organism might broadly affiliate the ZnD2sec gene with a spirochete (11). Here, without any interference from indirect phylogenetic hypothesis, direct single-cell analyses revealed an organism that would not have been on any previous list of candidates. This result raises the possibility that these deltaproteobacteria may play a major role in $H_2 + CO_2$ acetogenesis, which if true would substantially increase our understanding of bacterial acetogenesis in termites (8–11).

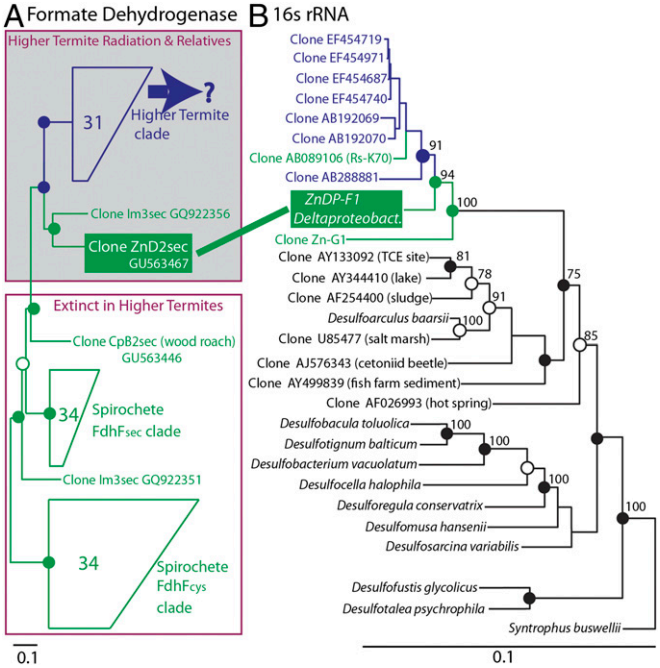

Fig. 1. Microfluidic digital PCR links a key FDH phylotype to a deltaproteobacterium. Phylograms of (*A*) deduced FDH protein and (*B*) 16s rRNA gene sequences. Sequences from evolutionarily lower termites and roaches are shown in green, and sequences recovered from higher termites are in blue. Higher termite FDH sequences group with the lower termite protozoan-associated fdh variant ZnD2sec (green box). Tree construction parameters and sequence accession numbers are listed in *SI Appendix*, Table S2. Each bar indicates 0.1 change per alignment position.

However, it remains possible that the species encoding ZnD2sec uses FDH in another anaerobic mode, such as pyruvate oxidation, purine fermentation (17), or interspecies formate transfer (18), all of which nevertheless would have relevance to mutualistic energy flow in the symbiosis. Hereinafter, we provisionally refer to the deltaproteobacterium expressing these ZnD2sec and SSU rRNA genes as genomovar ZnDP-F1.

HCR-FISH Localizes Genomovar ZnDP-F1–Expressing ZnD2sec mRNA and ZnDP-F1 rRNA to the Surface of a Protist. To independently >support the idea that genomovar ZnDP-F1 deltaproteobacteria encodes and coexpresses these mRNA and rRNA sequences, and to determine the exact association of these bacteria with specific particulates such as termite gut protozoa, we turned to a new multiplexed in situ hybridization technology based on the mechanism of hybridization chain reaction (HCR) (27). In this approach, mRNA and rRNA targets are detected using RNA probes that trigger hybridization cascades in which fluorophore-labeled RNA hairpins self-assemble into tethered fluorescent amplification polymers. Straightforward multiplexing follows from the simultaneous use of multiple HCR amplifiers programmed to operate independently.

We first performed three-channel colocalization studies in environmental bacterial samples isolated from homogenized termite gut samples (Fig. 2 and *SI Appendix*, Fig. S4). The ZnD2sec mRNA, the genomovar ZnDP-F1 rRNA, and the rRNA of all bacteria were targeted using single probes carrying different HCR initiators (Fig. 2 *A*–*C*). The composite image of Fig. 2*D* reveals strong signal colocalization for the ZnD2sec mRNA and the genomovar ZnDP-F1 deltaproteobacterial rRNA, with bacterial clusters stained either for both targets or for neither target. Staining for the rRNA of all bacteria confirmed that bacteria unstained for ZnD2sec mRNA and genomovar ZnDP-F1 rRNA were nonetheless amenable to HCR staining (Fig. 2*C*).

To gain further insight into these colocalization relationships, we applied a background threshold to the fluorescence in each channel to identify interesting pixels (Fig. 2 *G*–*I*), selected salient bacterial clusters with contrasting morphologies and costaining properties (orange rectangle, costaining for all three targets; blue rectangle, elongated spirochete-like morphology with predominant staining only for the rRNA of all bacteria), and created scatterplots of these pixel intensities for each pair of channels (Fig. 2 *J*–*L*). The results are striking. As shown in Fig. 2*J*, signals for the ZnD2sec mRNA and genomovar ZnDP-F1 deltaproteobacteria rRNA were minimal for the blue cluster and scaled linearly for the orange cluster. At high signal intensity, a subpopulation of pixels deviated from the linear relationship, exhibiting a disproportionate mRNA signal. Fig. 2*K* compares signals for the ZnD2sec mRNA and the rRNA of all bacteria, revealing a vertical blue distribution that reaffirms the absence of ZnD2sec staining for this elongated bacterial cluster. The predominant linear relationship, with a deviating subpopulation at high signal, is again evident for the orange cluster. Fig. 2*L* compares the signals for genomovar ZnDP-F1 rRNA and the rRNA of all bacteria, revealing linear relationships for both the orange and blue distributions. The blue scatter deviates slightly from vertical, suggesting that the ZnDP-F1 deltaproteobacteria rRNA probe may be binding with low efficiency to off-target rRNAs in the blue bacterial cluster. For the orange cluster, the clean linear relationship between the rRNA signals contrasts with the excursion from linearity of the rRNA vs. mRNA distributions of Fig. 2 *J* and *K*, suggesting that these excursions are likely biological rather than artifacts of the assay. Overall, the predominance of single linear relationships in the orange and blue distributions of Fig. 2 *J*–*L* suggests that the probes selectively bind single target sequences (*SI Appendix*, Figs. S8 and S9). The close correlation between ZnD2sec mRNA staining and genomovar ZnDP-F1 rRNA staining is consistent with expectations based on the foregoing microfluidics results.

To search for evidence of a spatial association between genomovar ZnDP-F1 deltaproteobacteria and termite gut protists,

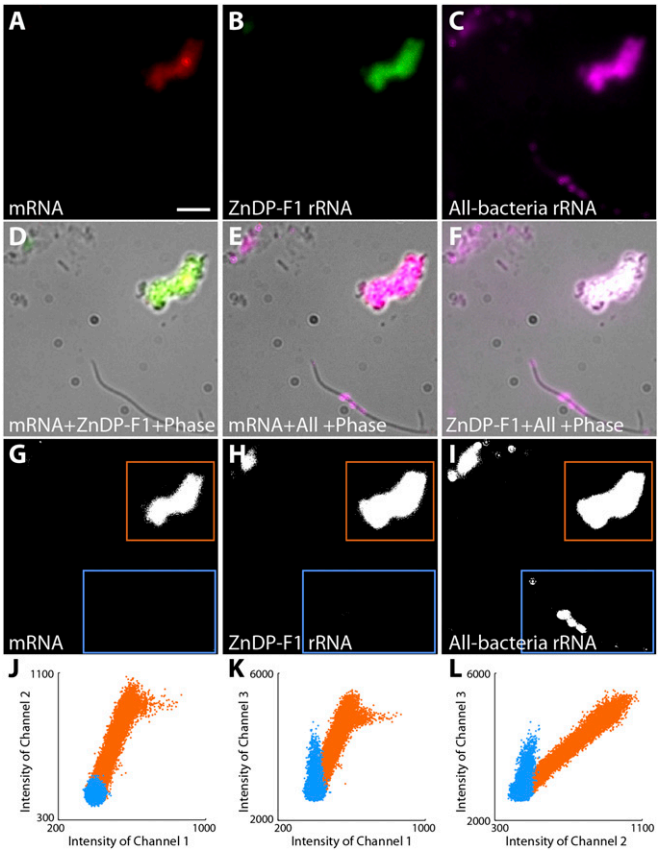

Fig. 2. Colocalization of ZnD2sec mRNA, ZnDP-F1 deltaproteobacterial rRNA, and the rRNA of all bacteria in lysed protozoal preparations. (*A*) Signal for ZnD2sec mRNA. (*B*) Signal for *ZnDP-F1*-rRNA. (*C*) Signal for rRNA of all bacteria. (*D*–*F*) Composite of each pair of channels with phase. (*G*–*I*) White pixels depict all areas in the image above a background threshold in a given channel. White pixels within the orange and blue rectangles are used for the scatterplots in *J*–*L*. (*J*–*L*) Scatterplots comparing pixel intensities for each pair of channels localized at each pixel within a given area. Orange and blue data are for bacterial clusters with contrasting morphologies and costaining properties. (Scale bar: 5 μm.) More samples shown in *SI Appendix*, Fig. S4.

we performed three-channel in situ HCR on particulate and protozoan-containing samples removed intact from *Zootermopsis* guts (Fig. 3 and *SI Appendix*, Fig. S5). The signal for the ZnD2sec mRNA colocalized with the signal for the ZnDP-F1 rRNA, and these signals were localized to protozoa resembling the *Z. nevadensis* protozoans *Trichonympha campanula* and *Trichonympha sphaerica* (based on morphology; Fig. 3 *A*–*C*). Our finding that not all rRNA-stained cells (or clusters of cells) stained with the mRNA probe is not surprising, considering the known differences in both the quantity and stability between bacterial mRNAs and rRNAs. Similar patterns, in which not all cells stained by rRNA probes stain with an mRNA probe, have been found in similar FISH experiments performed on single cells of laboratory-grown cultures (28) (*SI Appendix*, Fig. S9). The signal for the rRNA of all bacteria also colocalized with the signal from the ZnDP-F1 rRNA (Fig. 3 *D* and *E*). The high signal correlation using specific and general SSU rRNA probes suggests that this protist-associated bacterial niche may be dominated by a single deltaproteobacterial species.

The HCR-FISH data presented in Figs. 2 and 3 provide independent support for the microfluidic digital PCR data, with both indicating high expression of ZnD2sec by a previously unappreciated deltaproteobacterium, genomovar ZnDP-F1, which is associated with termite gut protozoa. This independent support for colocalization was not reported in previous studies using multiplexed microfluidic digital PCR (14, 20), owing largely to the

long-standing difficulty in visualizing mRNA expression in bacteria harvested from the environment (28). Here, using HCR-FISH, we were able to visualize multiple targets within bacterial cells harvested from the environment and measuring 0.3 × 0.6 μm, roughly 1/10th the volume of *Escherichia coli*.

Two additional independent studies support the localization of genomovar ZnDP-F1 deltaproteobacteria on *Trichonympha* protists. First, a metagenomic database compiled from cytoplasmic preparations of *Trichonympha* cells from *Z. nevadensis* guts optimized for recovery of the bacterial endosymbiont *Endomicrobium trichonymphae* (genome.jgi.doe.gov; GoldID Gm00182) clearly also contained small amounts of deltaproteobacterial DNA, in ~1,000 out of ~40,000 gene calls. One gene was found to be 99.9% identical to the ZnD2sec FDH gene, whereas another was 99.9% identical to the SSU RNA of genomovar ZnDP-F1. Second, a recent study of *Z. nevadensis* trichonymphas using micropipettes found associated bacterial SSU rRNA sequences that are 99% similar to the sequence of genomovar ZnDP-F1 (29).

Discussion

Taken together, the results of this study increase our understanding of bacteria expressing key genes of CO_2-reductive acetogenesis in the hindguts of the dampwood termite *Zootermopsis*. The guts of this insect exhibit high rates of this activity, which is highly relevant to the mutualistic, dietary symbiosis of termites (4, 5).

Protozoa as Niche. Diverse microbes attached to the surface of, or resident in the cytoplasm of, protozoa may compose a large fraction of the total gut bacterial load, considering that protozoa dominate up to 90% of the hindgut volume of lower termites (21). Previous studies have proposed roles for these bacteria (26, 30–32), but the challenges faced when studying their physiology in vitro or in situ makes many proposed interactions only speculative. Nonetheless, it has long been known that many termite gut protozoa produce H_2 as a fermentation product (1, 33), and thus direct interspecies hydrogen exchanges between protozoa and attached, epibiotic, H_2-consuming spirochetes has been hypothesized (8, 31). The present study provides direct genetic evidence of $H_2 + CO_2$ metabolic potential by a bacterial epibiont of a H_2-producing termite gut protozoan.

Presence of Genomovar ZnDP-F1–Like Deltaproteobacterial Ribotypes and Hydrogenase-Linked FDH Genes in Termites Wherein Gut Flagellate Protists Are Absent. Our results also have direct relevance to achieving a better understanding of lignocellulose processing by the most successful lineages of termites worldwide. In terms of total number of species and biomass, most termites are members of the family *Termitidae*, the so-called "higher" termites. Unlike all known species of the less-derived wood roaches (*Cryptocercus*) and "lower" termite families, all of which contain diverse cellulose-decomposing and other gut flagellates, higher termite gut communities are devoid of these flagellates (1, 12). With the loss of protozoa in ancestral higher termites, affects on ectosymbiotic and endosymbiotic or other bacteria metabolically connected to protozoa might be expected. Indeed, signals for sweeping bacterial gene losses were recently observed in hydrogenase-linked FDH diversity analyses in higher termites. Four of five major *fdh*F_{sec} and all known *Fdh*$_{cys}$ lineages observed in lower termites and the wood roach are absent in multiple species of higher termites (19). Protozoa-associated ZnDP-F1 deltaproteobacterial species, along with the genes that they encode, might have been predicted to be among those lost from higher termite gut systems; surprisingly, however, the loss of their genes was not observed. Genomovar ZnDP-F1–like deltaproteobacterial ribotypes have been documented in higher termite gut communities (Fig. 1) (12, 29). Moreover, ZnD2sec (the FDH type linked to ZnDP-F1 here) lies at the base of, and shares evolutionary relatedness to the exclusion of all other genes in the databases with, the single surviving lineage of FDH that has since radiated in higher termites (Fig. 1) (19). All other FDH lineages observed in other termites and the related wood roach, including those associated with spirochetes here or in other studies (11, 13, 19), are absent, and metagenomic analyses of higher termite gut communities (12, 34) have identified no alternative FDH candidates. Thus, to date, ZnD2sec-like FDHs remain the sole

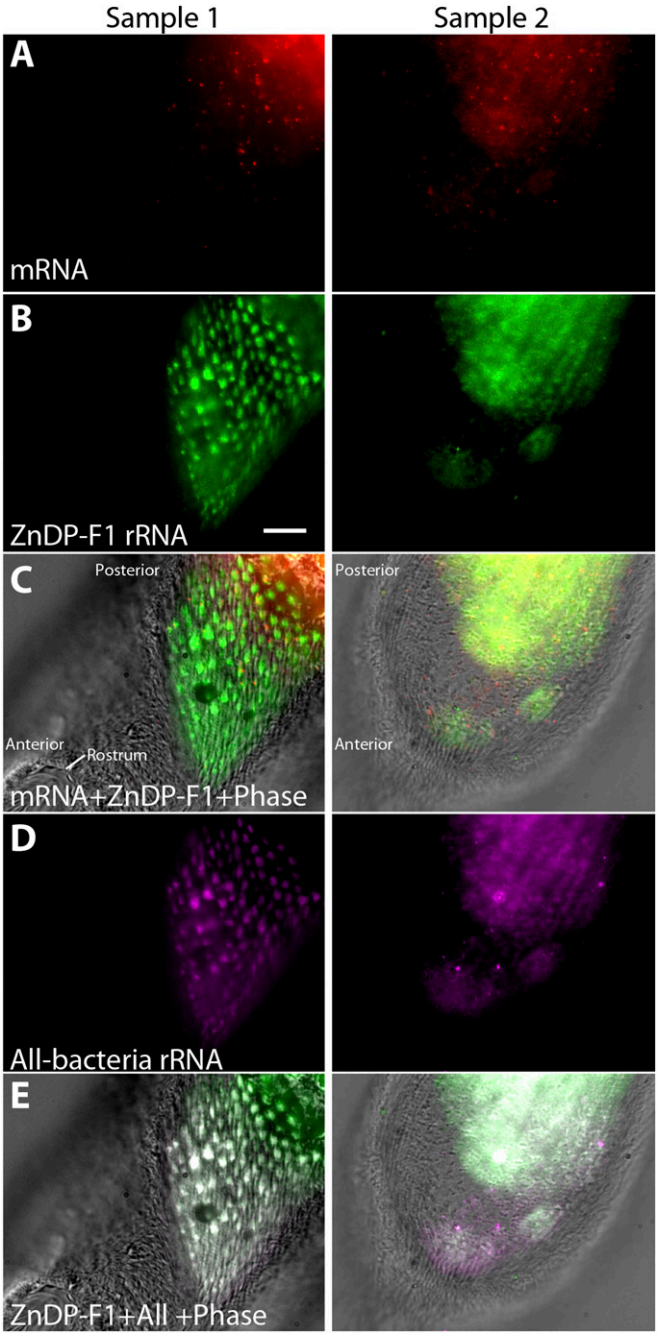

Fig. 3. Colocalization of ZnD2sec mRNA and ZnDP-F1 deltaproteobacteria rRNA in association with termite gut protozoa. Two different *Trichonympha*-like protozoans are shown, one protozoan per column. (*A*) Signal for ZnD2sec mRNA. Note the autofluorescent haze properties of protozoa in the upper right corner (posterior); a similar autofluorescent signal was seen in unstained samples (*SI Appendix*, Fig. S6). (*B*) Signal for ZnDP-F1 rRNA. (*C*) Composite of the ZnD2sec mRNA signal and ZnDP-F1 rRNA signal with phase contrast. (*D*) Signal for rRNA of all bacteria. (*E*) Composite of the ZnDP-F1 rRNA signal and all-bacteria rRNA signal with phase contrast. (Scale bar: 10 μm.) More samples in *SI Appendix*, Fig. S5 and Movie S1.

MICROBIOLOGY

candidate genes in higher termites for an important step in CO_2-reductive acetogenesis known to occur at high rates in all wood-feeding, higher termites examined (12, 35).

Our present results suggest the possibility that relatives of protozoan-associated ZnDP-F1 deltaprotebacteria succeeded in weathering a major environmental perturbation by making a major shift in their spatial niche in situ, that is, during the major events that led to loss of the protozoal community. Furthermore, their subsequent radiation into newly available, diverse acetogenic niches in the gut expanded their activities as major players in H_2 + CO_2 metabolism in higher termites (blue arrow hypothesis; Fig. 1). This possibility, guided by indirect phylogenetic inference, may be examined in the future using direct approaches similar to those applied here.

In conclusion, only a fraction of the available FTHFS and FDH genes were highly expressed in the microbial community of the host; for example, five or fewer bacterial species accounted for >85% of the observed FDH transcript pool (Table 1 and *SI Appendix*, Tables S3 and S4 and Figs. S2 and S3). One of these species is an active, uncultivated, and previously unappreciated deltaproteobacterium, and the other species are specific spirochetes encoding >30% of the FTHFS and FDH transcripts observed in the gut of *Zootermopsis*. These two different types live different lifestyles and occupy distinct spatial niches in situ, that is, swimming free in the luminal fluid vs. attached directly to H_2-producing cellulolytic protists. Confirmation of the latter association using HCR-FISH in a tiny deltaproteobacterium in its natural habitat opens many doors in environmental and medical microbiology, making it now tenable to localize in situ distinct transcripts expressed by important bacterial cells of interest.

Materials and Methods

Termite Collection. Worker *Z. nevadensis* termites were collected in the San Gabriel Mountains (California) and kept as detailed in *SI Appendix*.

RNA-Seq. Samples were prepared as described in *SI Appendix* and previously (36). Libraries were constructed and sequenced using the standard Illumina protocol and pipeline and aligned to inventories of FDH and FTHFS sequences. Details, controls, and validation are provided in *SI Appendix*.

Microfluidic Multiplex Digital PCR. Experiments were performed as described previously (14, 20). When particulates (pellet) samples were processed, the supernatant was discarded and pellets were resuspended in double-distilled H_2O, and repeatedly pipetted and lightly vortexed to disrupt large particles and protozoa. Probe information and reaction concentrations are provided in *SI Appendix*.

HCR-FISH. The HCR-FISH protocol was based on a previously described protocol (27). Modifications, probe and amplifier sequences and details of the protocol and experimental samples are provided in *SI Appendix*. Pixel intensities, the fluorescent value at each pixel of the field for each exposure (image), were calculated for all fluorescent channels.

ACKNOWLEDGMENTS. We thank Dr. Scott Fraser and staff at the Biological Imaging Center, Colby Calvert and staff at the Molecular Instruments Resource, Igor Antoscheckhin and staff at the Jacobs Genetics and Genomics Laboratory, and Drs. Eric Matson and Victoria Orphan for comments. Research support was provided by the US Department of Energy (Grant DE-FG02-07ER64484), the Center for Environmental Microbial Interactions at Caltech, the National Institutes of Health (Grant 5R01 EB006192, to H.M.T.C. and N.A.P.), the Beckman Institute at Caltech (H.M.T.C. and N.A.P.), and a Caltech Rosen Center Bioengineering Scholarship (to V.T.).

1. Abe T, Bignell DE, Higashi M (2000) *Termites: Evolution, Sociality, Symbioses, Ecology* (Kluwer Academic, Dordrecht), pp 1–42.
2. Breznak JA, Kane MD (1990) Microbial H_2/CO_2 acetogenesis in animal guts: Nature and nutritional significance. *FEMS Microbiol Rev* 7(3-4):309–313.
3. Shively JM, English RS, Baker SH, Cannon GC (2001) Carbon cycling: The prokaryotic contribution. *Curr Opin Microbiol* 4(3):301–306.
4. Breznak JA, Switzer JM (1986) Acetate synthesis from H_2 plus CO_2 by termite gut microbes. *Appl Environ Microbiol* 52(4):623–630.
5. Pester M, Brune A (2007) Hydrogen is the central free intermediate during lignocellulose degradation by termite gut symbionts. *ISME J* 1(6):551–565.
6. Pester M, Brune A (2006) Expression profiles of fhs (FTHFS) genes support the hypothesis that spirochaetes dominate reductive acetogenesis in the hindgut of lower termites. *Environ Microbiol* 8(7):1261–1270.
7. Kane MD, Breznak JA (1991) *Acetonema longum* gen. nov. sp. nov., an H_2/CO_2 acetogenic bacterium from the termite, *Pterotermes occidentis*. *Arch Microbiol* 156(2): 91–98.
8. Leadbetter JR, Schmidt TM, Graber JR, Breznak JA (1999) Acetogenesis from H_2 plus CO_2 by spirochetes from termite guts. *Science* 283(5402):686–689.
9. Ottesen EA, Leadbetter JR (2010) Diversity of formyltetrahydrofolate synthetases in the guts of the wood-feeding cockroach *Cryptocercus punctulatus* and the omnivorous cockroach *Periplaneta americana*. *Appl Environ Microbiol* 76(14):4909–4913.
10. Salmassi TM, Leadbetter JR (2003) Analysis of genes of tetrahydrofolate-dependent metabolism from cultivated spirochaetes and the gut community of the termite *Zootermopsis angusticollis*. *Microbiology* 149(Pt 9):2529–2537.
11. Zhang X, Matson EG, Leadbetter JR (2011) Genes for selenium-dependent and independent formate dehydrogenase in the gut microbial communities of three lower, wood-feeding termites and a wood-feeding roach. *Environ Microbiol* 13(2):307–323.
12. Warnecke F, et al. (2007) Metagenomic and functional analysis of hindgut microbiota of a wood-feeding higher termite. *Nature* 450(7169):560–565.
13. Matson EG, Zhang X, Leadbetter JR (2010) Selenium controls transcription of paralogous formate dehydrogenase genes in the termite gut acetogen, *Treponema primitia*. *Environ Microbiol* 12(8):2245–2258.
14. Ottesen EA, Hong JW, Quake SR, Leadbetter JR (2006) Microfluidic digital PCR enables multigene analysis of individual environmental bacteria. *Science* 314(5804): 1464–1467.
15. Ragsdale SW, Pierce E (2008) Acetogenesis and the Wood-Ljungdahl pathway of $CO_(2)$ fixation. *Biochim Biophys Acta* 1784(12):1873–1898.
16. Zinoni F, Birkmann A, Stadtman TC, Böck A (1986) Nucleotide sequence and expression of the selenocysteine-containing polypeptide of formate dehydrogenase (formate-hydrogen-lyase-linked) from *Escherichia coli*. *Proc Natl Acad Sci USA* 83(13): 4650–4654.
17. Thauer RK (1973) CO_2 reduction to formate in *Clostridium acidi-urici*. *J Bacteriol* 114(1):443–444.
18. Stams AJ, Plugge CM (2009) Electron transfer in syntrophic communities of anaerobic bacteria and archaea. *Nat Rev Microbiol* 7(8):568–577.
19. Zhang X, Leadbetter JR (2012) Evidence for cascades of perturbation and adaptation in the metabolic genes of higher termite gut symbionts. *mBio* 3(4), e00223-12.
20. Tadmor AD, Ottesen EA, Leadbetter JR, Phillips R (2011) Probing individual environmental bacteria for viruses by using microfluidic digital PCR. *Science* 333(6038):58–62.
21. Berchtold M, et al. (1999) Differential enumeration and in situ localization of microorganisms in the hindgut of the lower termite *Mastotermes darwiniensis* by hybridization with rRNA-targeted probes. *Arch Microbiol* 172(6):407–416.
22. Leadbetter JR, Breznak JA (1996) Physiological ecology of *Methanobrevibacter cuticularis* sp. nov. and *Methanobrevibacter curvatus* sp. nov., isolated from the hindgut of the termite *Reticulitermes flavipes*. *Appl Environ Microbiol* 62(10):3620–3631.
23. Ohkuma M (2008) Symbioses of flagellates and prokaryotes in the gut of lower termites. *Trends Microbiol* 16(7):345–352.
24. Schink B, Thiemann V, Laue H, Friedrich MW (2002) *Desulfotignum phosphitoxidans* sp. nov., a new marine sulfate reducer that oxidizes phosphite to phosphate. *Arch Microbiol* 177(5):381–391.
25. Jansen K, Fuchs G, Thauer RK (1985) Autotrophic CO_2 fixation by *Desulfovibrio baarsii*: Demonstration of enzyme-activities characteristic for the acetyl-CoA pathway. *FEMS Microbiol Lett* 28(3):311–315.
26. Sato T, et al. (2009) Candidatus *Desulfovibrio trichonymphae*, a novel intracellular symbiont of the flagellate *Trichonympha agilis* in termite gut. *Environ Microbiol* 11(4):1007–1015.
27. Choi HMT, et al. (2010) Programmable in situ amplification for multiplexed imaging of mRNA expression. *Nat Biotechnol* 28(11):1208–1212.
28. Pernthaler A, Amann R (2004) Simultaneous fluorescence in situ hybridization of mRNA and rRNA in environmental bacteria. *Appl Environ Microbiol* 70(9):5426–5433.
29. Strassert JF, et al. (2012) "*Candidatus* Ancillula trichonymphae," a novel lineage of endosymbiotic *Actinobacteria* in termite gut flagellates of the genus *Trichonympha*. *Environ Microbiol* 14(12):3259–3270.
30. Hongoh Y, et al. (2008) Complete genome of the uncultured Termite Group 1 bacteria in a single host protist cell. *Proc Natl Acad Sci USA* 105(14):5555–5560.
31. Hongoh Y, et al. (2008) Genome of an endosymbiont coupling N_2 fixation to cellulolysis within protist cells in termite gut. *Science* 322(5904):1108–1109.
32. Noda S, Hongoh Y, Sato T, Ohkuma M (2009) Complex coevolutionary history of symbiotic Bacteroidales bacteria of various protists in the gut of termites. *BMC Evol Biol* 9:158.
33. Odelson DA, Breznak JA (1983) Volatile fatty acid production by the hindgut microbiota of xylophagous termites. *Appl Environ Microbiol* 45(5):1602–1613.
34. He S, et al. (2013) Comparative metagenomic and metatranscriptomic analysis of hindgut paunch microbiota in wood- and dung-feeding higher termites. *PLoS ONE* 8(4):e61126.
35. Brauman A, Kane MD, Labat M, Breznak JA (1992) Genesis of acetate and methane by gut bacteria of nutritionally diverse termites. *Science* 257(5075):1384–1387.
36. Rosenthal AZ, Matson EG, Eldar A, Leadbetter JR (2011) RNA-Seq reveals cooperative metabolic interactions between two termite-gut spirochete species in co-culture. *ISME J* 5(7):1133–1142.